ACS OMEGA

Open Access

http://pubs.acs.org/journal/acsodf

Article

Study on the Continuous Whole Process Preparation of Peptizable Pseudoboehmite by High Gravity Strengthening Reaction of CO_2 and Heat Transfer

Chengqian Zhang, Youzhi Liu,* Yuliang Li, Shuwei Guo, Shufei Wang, and Shangyuan Cheng

Cite This: *ACS Omega* 2024, 9, 43570−43582

Read Online

ACCESS | Metrics & More | Article Recommendations

ABSTRACT: The preparation of highly peptizable pseudoboehmite faces challenges such as slow reaction rate, prolonged aging times leading to poor peptization performance, and difficulty in achieving continuous production. In this study, a novel approach was proposed involving a high gravity reactor to enhance carbonation reaction control for pseudoboehmite nucleation, a high gravity steam heating process, and a continuous aging process in pipelines. By coupling these three processes, the continuous whole process production of highly peptizable pseudoboehmite under high gravity conditions was achieved. First, the effect of high gravity reactor enhancement on the reaction and the resulting solid phase was investigated. Second, the impact of aging temperature and time on the solid phase formed at different reaction end points was studied using high gravity and steam heating of the liquid phase. Furthermore, the influence of synthesis conditions on the peptization performance of pseudoboehmite was extensively examined. Finally, the nucleation and growth mechanisms of pseudoboehmite under high gravity conditions were analyzed. It was found that increasing high gravity factor, CO_2 gas flow rate, and CO_2 content accelerated carbonation reaction rate, promoting pseudoboehmite crystal nucleation. Increasing aging temperature and time facilitated the growth of pseudoboehmite nuclei and improved peptization performance. The high gravity device altered the gas−liquid phase contact state of traditional kettle-type equipment, reducing the reaction time and heating time from minutes to seconds, thus achieving the continuous whole process production of pseudoboehmite with a peptization index of 100% from sodium aluminate solution by kiln flue gas.

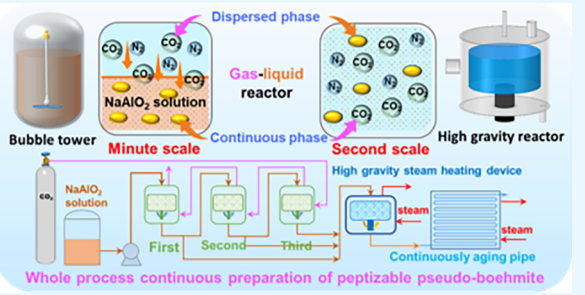

1. INTRODUCTION

Pseudoboehmite, a crystalline form of aluminum hydroxide, serves as a precursor to active alumina and is a crucial product in wet metallurgy. It finds extensive applications in various industries such as chemical engineering,[1−6] environmental protection,[7−10] energy,[11,12] and medical sectors.[13−16] Notably, pseudoboehmite possesses desirable pore structures, making it suitable for use as a catalyst support and adsorbent. Moreover, under certain acidic conditions, it can gel into viscoelastic materials, exhibiting excellent peptization properties, which renders it valuable as a binder[17−19] for catalysts and adsorbents, facilitating their shaping. While significant research[20−23] efforts have been directed toward producing pseudoboehmite with large pore volumes, there is a dearth of studies focusing on the preparation of pseudoboehmite with high peptization performance.

The methods for preparing pseudoboehmite encompass acid-based,[24−28] alkali-based,[29−31] carbonation,[32,33] dual-aluminum,[34,35] and alcohol-aluminum techniques.[36−39] Among these, the carbonation method stands out for its utilization of sodium aluminate solution, an intermediate derived from alumina refining, and kiln exhaust rich in carbon dioxide. Notably, this process offers environmental benefits, as the resulting wastewater can be recycled, enhancing its overall sustainability and cost-effectiveness. However, studies[22,23,33,40] have highlighted a drawback: the propensity of the carbonation reaction to yield undesirable crystalline phases of aluminum hydroxide. It is given that aluminum hydroxide exhibits various crystal phases that readily convert between each other. Aluminum hydroxides of other crystalline phases lack peptization properties. Consequently, meticulous control over crystal nucleation and growth during the carbonation reaction emerges as a pivotal concern in the quest for highly peptizable pseudoboehmite.

Previous studies have extensively investigated the synthesis of pseudoboehmite crystals. Lu et al.[21] demonstrated the crucial role of the final pH in the carbonation reaction in

Received: June 14, 2024
Revised: October 5, 2024
Accepted: October 8, 2024
Published: October 16, 2024

https://doi.org/10.1021/acsomega.4c05591
ACS Omega 2024, 9, 43570−43582

determining the crystal phase. Furthermore, Zhang et al.[41] elucidated that the concentration of sodium aluminate solution governs the critical end point pH for pseudoboehmite synthesis during the carbonation process. An increase in the sodium aluminate solution concentration results in an expansion of the critical end point pH value. The research findings of Ren et al.[42] and Chen et al.[43] both corroborate the notion that the end point pH determines the crystal phase of aluminum hydroxide. Specific researchers[21] observed that bayerite forms with 25% carbon dioxide content, whereas pseudoboehmite forms with 35% carbon dioxide content. Therefore, it can be inferred that accelerating the carbonation reaction rate also significantly affects the nucleation of pseudoboehmite. Previous researchers have long believed that the carbonation reaction at elevated temperatures leads to the formation of bayerite. Shayanfar et al.[44,45] reported that bayerite precipitates through the carbonation reaction at pH = 11 within the temperature range of 50−90 °C. Consequently, crucial factors in regulating crystal nucleation during the carbonation reaction include enhancing the reaction rate at low temperatures and precisely controlling the end point pH of the reaction.

The control of nucleation in the carbonation reaction relies on reactors. Several studies[33,46−48] have indicated that the reaction time for pseudoboehmite preparation using bubble column reactors exceeds 20 min. Chinese enterprises commonly employ bubble column reactors for batch production, with reaction times typically ranging from 15 to 30 min. To mitigate this, previous research has investigated intensified techniques in the carbonation method for pseudoboehmite synthesis. Numerous studies have demonstrated the preparation of large pore pseudoboehmite using membrane dispersion coupled with microreactors,[23,33] achieving a batch reaction time of 8 min for a 0.2 mol/L sodium aluminate solution. Chen et al.[43,49,50] utilized high gravity technology to enhance the carbonation reaction of a 0.1 mol/L sodium aluminate solution, reducing the batch reaction time from 15 to 8 min and successfully producing nanofibrous and sheet-like aluminum hydroxide. Despite these advancements, studies still involve batch reactions with prolonged reaction times and high production costs. Therefore, further research into intensified reaction technologies to expedite carbonation reactions for continuous production processes is of paramount importance for both academic research and industrial applications. While high gravity technology, as reported, has not yet achieved control over crystal nucleation and continuous production processes in the carbonation reaction, its unique characteristics surpass those of other intensification methods, warranting further investigation.

High gravity technology[51] is one of the most promising branches of process intensification (PI), which is carried out in a rotating packed bed (RPB) and has been applied to deaeration, distillation, reaction, absorption, mass transfer, nanoparticle preparation, and so on. The high-speed rotating packing driven by the motor shears the liquid into tiny droplets, filaments, and liquid membranes, which provides intense microscopic mixing for the gas−liquid two-phase fluid and intensifies the mass transfer process.

Numerous researchers[29,44,45,50] have shown that the conditions of the carbonation reaction not only affect the pore structure of pseudoboehmite, but the aging temperature and duration also significantly influence its pore morphology. Consequently, aging conditions may also affect the peptization efficacy of pseudoboehmite. Several studies[22,46,49] have reported the use of water bath heating for aging. In industrial settings, steam is directly used to heat the slurry in a tank. Both of these aging methods are intermittent and plagued by issues, such as prolonged heating periods, temperature fluctuations, and uneven aging durations. The aging process profoundly impacts the growth of pseudoboehmite crystals and their peptization characteristics, thereby imposing constraints on the entire continuous production process.

To address the issues of slow carbonation reaction rate leading to the difficulty in preparing highly peptizable pseudoboehmite, prolonged aging heating time, and low efficiency of batch production, this study proposed a method involving a high gravity reactor to enhance the carbonation reaction for controlling the pseudoboehmite nucleation process, high gravity steam heating process, and continuous pipeline aging process. The coupling of these three methods achieved the continuous whole process preparation of highly peptizable pseudoboehmite. First, the influence of high gravity reaction conditions on the reaction end point and reaction time was investigated, including the high gravity factor, gas−liquid ratio, gas concentration, and reaction frequency. Simultaneously, the solid phase was examined. Second, using high gravity and steam heating of the liquid material, the effects of aging temperature and time on the solid phase formed at different reaction end points were studied. Furthermore, a detailed investigation was conducted on the effects of carbonation reaction conditions and aging conditions under a high gravity environment on the peptization performance of pseudoboehmite. Finally, the nucleation and growth mechanisms of pseudoboehmite under a high gravity field were analyzed.

2. EXPERIMENTAL SECTION

2.1. Material. Sodium aluminate solids were purchased from Tianjin Damao Chemical Reagent Factory. Deionized (DI) water used in all experiments was obtained from a Purifier ultrapure water system. The purity of carbon dioxide gas and nitrogen used in the experiment was 99.9%, which were purchased from Taiyuan Taineng Gas Co., Ltd. Three counter-flow high gravity reactors (the rotating packed bed)[52] and high gravity steam heated device were made in the laboratory. The four high gravity devices have rotors with a height of 20 mm, a diameter of 400 mm, an inner diameter of 60 mm, and a packing porosity of 55%. The continuous aging pipe was a PVC hose with a diameter of 60 mm and a length of 32 m. The pipe was placed in a spiral and fixed in a closed incubator. The pipe inlet was below, and the outlet was above. The liquid flowed from the bottom up. The outlet height of the continuously aged pipe was lower than that of the high gravity device.

2.2. Procedures. The experimental setup for the continuous whole process preparation of pseudoboehmite is illustrated in Figure 1, comprising three high gravity reactors, a high gravity steam heating device, continuous aging pipelines, storage tanks, peristaltic pumps, and gas cylinders. The experimental procedure involved the sodium aluminate solution being conveyed to the first high gravity reactor by a peristaltic pump and then sequentially passing through the second and third reactors. Carbon dioxide gas entered the first, second, and third reactors through flow meters. The sodium aluminate solution reacted with carbon dioxide gas in the reactors to produce pseudoboehmite slurry. The slurry was

https://doi.org/10.1021/acsomega.4c05591
ACS Omega 2024, 9, 43570−43582

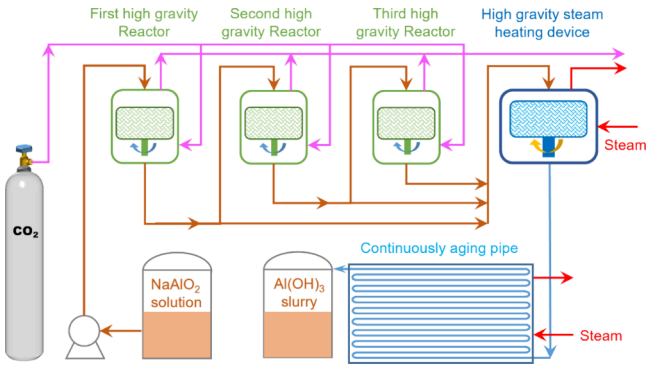

Figure 1. Experimental setup for the continuous whole process preparation of pseudoboehmite.

rapidly heated to the aging temperature by steam in the high gravity steam heating device and then flowed at a constant temperature for a certain time (aging time) in the continuous aging pipeline. Nitrogen was used to configure carbon dioxide gas with different volume fractions. The steam temperature was 150 °C. When the heating temperature was 90 °C, the required steam flows were 70 g/min, 55 g/min at 70 °C, and 39 g/min at 70 °C. The aging time was adjusted by controlling the flow rate. After aging, the slurry was filtered, washed, and dried to obtain a powder. Drying was conducted at 110 °C for 6 h. The process of continuous preparation of pseudoboehmite powder is illustrated in Figure 2. The high gravity factor (β) was determined by the size and speed of the rotating packed bed. The calculation method for the high gravity factor was detailed in ref 51.

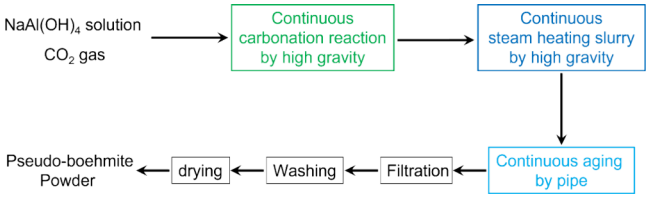

Figure 2. Process of continuous preparation of pseudoboehmite powder.

2.3. Characterization. To identify the crystal phase, the powder was characterized by an X-ray diffractometer and Fourier transform infrared spectrometer (FTIR, PerkinElmer, Waltham, Massachusetts, USA). Powder X-ray diffraction (XRD) patterns were recorded using a Rigaku Ultima IV with Cu KR (40 kV and 200 mA) between 5 and 85° at a scan speed of 8°/min. Thermogravimetry differential thermal analysis (TG−DTA) was carried out using a NETZSCH STA449F3. The morphologies of particles and membranes were observed using scanning electron microscopy (SEM, JEM-6301F Japan).

The test method of the gelatinization index of pseudoboehmite was as follows: A turbid liquid with a 10% Al_2O_3 content was formed by mixing pseudoboehmite containing 1.0000 g of Al_2O_3 with deionized water. Concentrated nitric acid (0.2 g) was added into the turbid liquid and shaken for 15 min and centrifuged for 15 min. The supernatant (5 mL) was calcined for 2 h at 550 °C, and the solid mass of Al_2O_3 after calcination was weighed. The solid after roasting of the supernatant is the alumina contained in the peptizable pseudoboehmite. The peptization index was calculated as 2 times the ratio of the residual solid mass of the calcined 5 mL supernatant to the mass of Al_2O_3 in the pseudoboehmite weighed.

3. RESULTS AND DISCUSSION

3.1. High Gravity-Enhanced Carbonization Reaction for Continuous Control of Pseudoboehmite Crystal Nucleation. This section focused solely on studying the aluminum hydroxide crystals generated by the carbonation reaction without undergoing an aging treatment. Zhang et al.[41] demonstrated that after 0.5 h at room temperature following the carbonation reaction, the absence of bayerite precipitation indicated the potential preparation of pseudoboehmite. Therefore, the crystalline phases of the precipitates formed 0.5 h after the carbonation reaction were also investigated.

3.1.1. Influence of High Gravity Factor on Reaction End Point pH and Crystal Phase. The high gravity factor (β) reflected the dispersion of liquid in the gravity reactor. Table 1 presents the experimental conditions and results corresponding to various high gravity factors. Figure 3 illustrates the influence of the high gravity factor on the end point pH of the sodium aluminate solution carbonation reaction. Furthermore, X-ray

Table 1. Experimental Result Table of the Effect of High Gravity Factor on Carbonation Reaction End Point pH_R and Crystals[a]

numbers	c_{NaAlO2}/(mol/L)	pH_0	β	ϕ_{CO2}/%	Q/L	L/(mL/min)	pH_{R1}	t_p/h	crystalline phase
1	0.1	12.92 ± 0.02	0	100	6:1	500	12.87 ± 0.04		N/A
2	0.1	12.92 ± 0.02	10	100	6:1	500	12.52 ± 0.03	0	N/A
3	0.1	12.92 ± 0.02	10	100	6:1	500	12.52 ± 0.03	0.5	N/A
4	0.1	12.92 ± 0.02	20	100	6:1	500	11.28 ± 0.03	0	AA
5	0.1	12.92 ± 0.02	20	100	6:1	500	11.28 ± 0.03	0.5	B
6	0.1	12.92 ± 0.02	40	100	6:1	500	10.75 ± 0.02	0	AA
7	0.1	12.92 ± 0.02	40	100	6:1	500	10.75 ± 0.02	0.5	B
8	0.1	12.92 ± 0.02	60	100	6:1	500	10.13 ± 0.02	0	AA
9	0.1	12.92 ± 0.02	60	100	6:1	500	10.13 ± 0.02	0.5	AA
10	0.1	12.92 ± 0.02	80	100	6:1	500	9.88 ± 0.02	0	AA
11	0.1	12.92 ± 0.02	80	100	6:1	500	9.88 ± 0.02	0.5	AA
12	0.1	12.92 ± 0.02	100	100	6:1	500	10.02 ± 0.03	0	AA

[a]pH_0: pH of the sodium aluminate solution before the reaction; β: high gravity factor; ϕ_{CO2}: carbon dioxide content in gas, %; Q/L: gas−liquid flow ratio; pH_{R1}: reaction end point of the first reactor; t_p: residence time in aging pipes; N/A: not enough solid precipitated for analysis; AA: amorphous aluminum hydroxide; B: bayerite. Reaction temperature T_R = 25 °C.

https://doi.org/10.1021/acsomega.4c05591
ACS Omega 2024, 9, 43570−43582

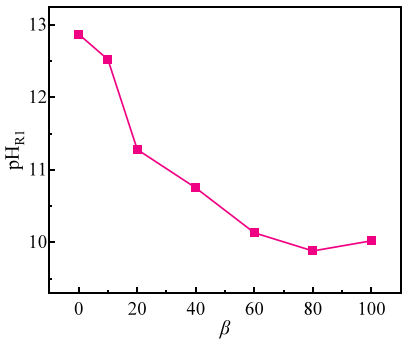

Figure 3. Effect of the high gravity factor on carbonation reaction end point pH_R.

diffraction (XRD) was utilized to characterize the crystal phase, as depicted in Figure 4. An observed trend with the increase in the high gravity factor was the initial decrease followed by an increase in the end point pH. A high gravity factor of 0 indicated negligible dispersion effects within the reactor, resulting in a minimal gas−liquid contact area, a small reaction volume, and only a slight decrease in pH, thereby preventing solid formation. At a high gravity factor of 10, the pH remained at 12.58, with no solid formation. However, for factors of 20 and 40, the pH decreased to 11.28 and 10.75, respectively, leading to the formation of amorphous aluminum hydroxide crystals. Subsequently, after a 0.5 h aging period in the pipe, bayerite crystals[53] (JCPDS no. 20-0011) were produced. When the high gravity factors increased to 60 and 80, the pH further decreased to 10.13 and 9.88, respectively, resulting in the formation of amorphous aluminum hydroxide crystals. However, no bayerite crystals were formed after the same aging period. The highest enhancement in the reaction was observed at a high gravity factor of 80, corresponding to the smallest pH_R. Surprisingly, at a factor of 100, the pH_R was not at its minimum. This phenomenon may have been attributed to the accelerated movement speed of the liquid and the reduced gas−liquid reaction time under extremely high gravity factors. The infrared spectrum findings were consistent with those obtained from XRD. The characteristic infrared absorption peaks[54] of bayerite were identified at wavelengths of 3657 and 3551 cm^{-1}, as shown in Figure 5. The band at 1450 cm^{-1} is for carbonate, so it indicates the presence of carbonates on the surface of bayerite.

Research revealed that high gravity significantly enhanced the carbonation reaction. As the high gravity coefficient increased, the gas−liquid mass transfer area enlarged, accelerating the carbonation reaction rate and significantly reducing the reaction time. At higher end point pH values, amorphous aluminum hydroxide was initially formed followed by the cessation of the carbonation reaction and subsequent formation of bayerite. Conversely, at lower end point pH values, only amorphous aluminum hydroxide was generated. These findings aligned with those of Zhang et al.,[41] suggesting that higher end point pH values led to further decomposition of sodium aluminate in the solution, forming bayerite. Rapid reduction of the end point pH prevented bayerite crystal nucleation. Therefore, increasing the high gravity factor promoted the nucleation of amorphous aluminum hydroxide in the carbonation reaction, effectively suppressing bayerite nucleation. With a carbon dioxide gas volume fraction of 100%, continuous preparation of pseudoboehmite was achieved using a primary high gravity reactor.

3.1.2. Influence of Carbon Dioxide Volume Fraction on Reaction End Point pH and Crystal Phase. Table 2 presents the experimental conditions and results for various carbon dioxide volume fractions. Figure 6 illustrates the effect of carbon dioxide volume fraction on the end point pH_R of the carbonation reaction. The XRD characterization of the crystal phase is shown in Figure 7A. When carbon dioxide volume fractions were 20 and 40%, the pH decreased slightly, and the carbonation reaction rate was low, resulting in end point pH_R values of 12.73 and 12.51, respectively, with no crystal formation. As the carbon dioxide volume fraction increased, the pH decreased more rapidly and the carbonation reaction rate accelerated. When the end point pH of the carbonation reaction was 11.67, almost no solids were produced immediately after the reaction, but bayerite crystals formed after standing at room temperature for 0.5 h. When the end point pH was 10.5, amorphous aluminum hydroxide initially formed, and bayerite crystals formed after standing at room temperature for 0.5 h. The previous section discussed the experimental conditions with a carbon dioxide volume fraction of 100%. The experimental results indicated that increasing the carbon dioxide volume fraction accelerated the carbonation reaction rate, inhibited the decomposition of bayerite, and promoted the formation of amorphous aluminum hydroxide nuclei. By adjusting the carbon dioxide volume fraction to rapidly reduce the end point pH of the carbonation reaction, the nucleation of aluminum hydroxide generated from the carbonation reaction can be controlled. The infrared spectrum

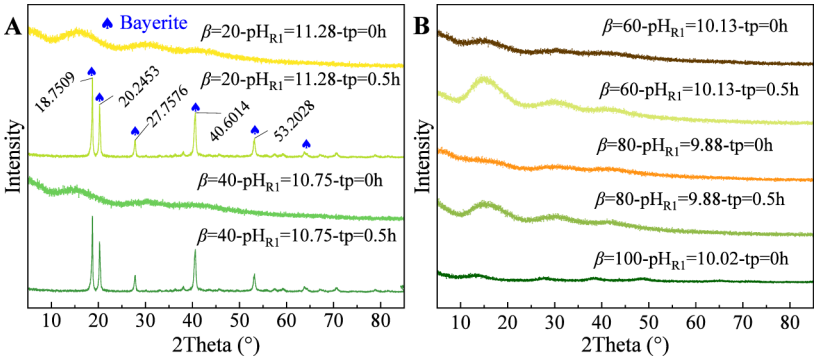

Figure 4. XRD pattern of precipitation generated by the first high gravity reactor. (A) The supergravity factors are 20 and 40. (B) The supergravity factors are 60, 80, and 100.

https://doi.org/10.1021/acsomega.4c05591
ACS Omega 2024, 9, 43570−43582

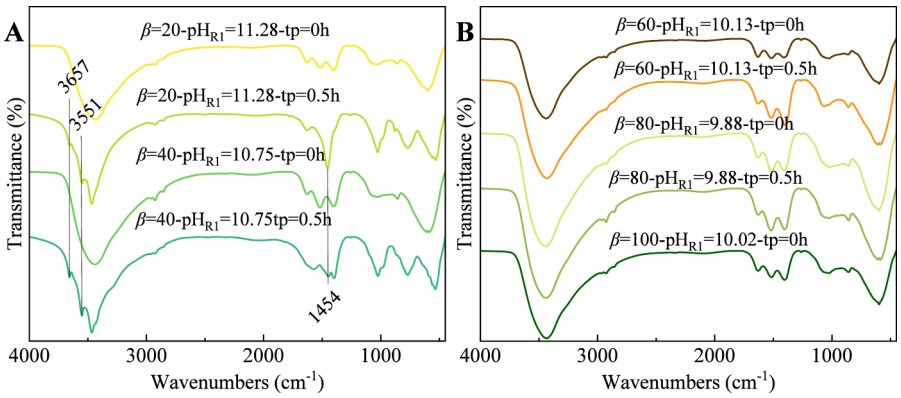

Figure 5. FTIR spectra of precipitation generated by the first high gravity reactor. (A) The supergravity factors are 20 and 40. (B) The supergravity factors are 60, 80, and 100.

Table 2. Experimental Result Table of the Effect of the Carbon Dioxide Content on Carbonation Reaction End Point pH$_R$ and Crystals

numbers	c_{NaAlO2}/(mol/L)	pH$_0$	β	ϕ_{CO2}/%	Q/L	L/(mL/min)	pH$_{R1}$	t_p/h	crystalline phase
13	0.1	12.92 ± 0.02	80	20	6:1	500	12.73 ± 0.04	0	N/A
14	0.1	12.92 ± 0.02	80	40	6:1	500	12.51 ± 0.03	0	N/A
15	0.1	12.92 ± 0.02	80	40	6:1	500	12.51 ± 0.03	0.5	N/A
16	0.1	12.92 ± 0.02	80	60	6:1	500	11.67 ± 0.01	0	N/A
17	0.1	12.92 ± 0.02	80	60	6:1	500	11.67 ± 0.01	0.5	B
18	0.1	12.92 ± 0.02	80	80	6:1	500	10.50 ± 0.02	0	AA
19	0.1	12.92 ± 0.02	80	80	6:1	500	10.50 ± 0.02	0.5	B

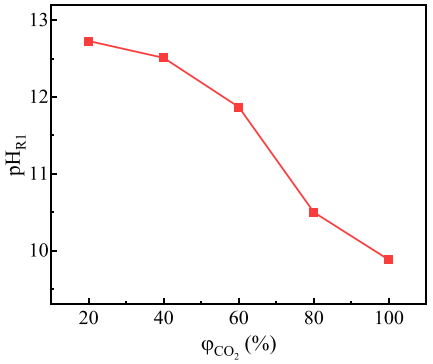

Figure 6. Effect of the carbon dioxide content on carbonation reaction end point pH$_R$.

findings were consistent with those obtained from XRD, as shown in Figure 7B.

3.1.3. Influence of the Gas−Liquid Flow Ratio on Reaction End Point pH and Crystal Phase. In industrial production, kiln flue gas with a carbon dioxide volume fraction of approximately 40% is typically used. Therefore, studying the impact of the gas−liquid flow ratio (Q/L) under the condition of 40% carbon dioxide volume fraction is of significant importance for both industrial applications and scientific research. The experimental conditions and results for different gas−liquid flow ratios are shown in Table 3. The effect of the gas−liquid flow ratio on the end point pH$_R$ of the carbonation reaction is illustrated in Figure 8, while the XRD and FTIR characterization results of the crystal phase are presented in Figure 9.

As the gas−liquid flow ratio increased, the end point pH$_R$ initially decreased and then increased. When the gas−liquid flow ratios were 2:1, 4:1, and 6:1, the amount of carbon dioxide was relatively small, resulting in a low carbonation reaction rate and relatively high end point pH values of 12.83,

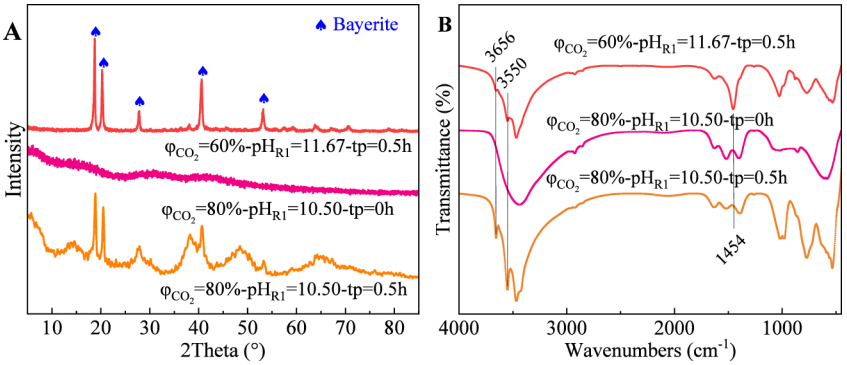

Figure 7. XRD pattern and FTIR spectra of precipitation generated by carbonation reaction (carbon dioxide content). (A) XRD pattern. (B) FTIR spectra.

https://doi.org/10.1021/acsomega.4c05591
ACS Omega 2024, 9, 43570−43582

Table 3. Experimental Result Table of the Effect of the Gas−Liquid Flow Ratio on Carbonation Reaction End Point pH_R and Crystals

numbers	c_{NaAlO2}/(mol/L)	pH_0	β	ϕ_{CO2}/%	Q/L	L/(mL/min)	pH_{R1}	t_p/h	crystalline phase
20	0.1	12.92 ± 0.02	80	40	2:1	500	12.83 ± 0.03	0	N/A
21	0.1	12.92 ± 0.02	80	40	4:1	500	12.68 ± 0.02	0	N/A
22	0.1	12.92 ± 0.02	80	40	8:1	500	11.86 ± 0.03	0	N/A
23	0.1	12.92 ± 0.02	80	40	8:1	500	11.86 ± 0.03	0.5	B
24	0.1	12.92 ± 0.02	80	40	10:1	500	11.17 ± 0.02	0	
25	0.1	12.92 ± 0.02	80	40	12:1	500	10.87 ± 0.02	0	AA
26	0.1	12.92 ± 0.02	80	40	12:1	500	10.87 ± 0.02	0.5	B
27	0.1	12.92 ± 0.02	80	40	14:1	500	10.93 ± 0.03	0	
28	0.1	12.92 ± 0.02	80	40	16:1	500	11.02 ± 0.02	0	

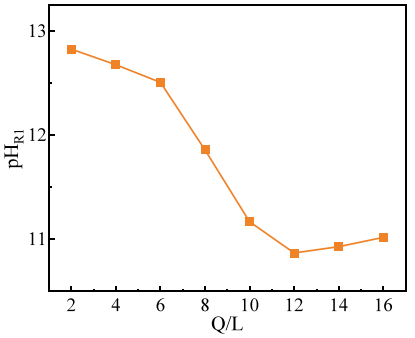

Figure 8. Effect of the gas−liquid flow ratio on carbonation reaction end point pH_R.

12.68, and 12.51, respectively. Under these conditions, no decomposition of sodium aluminate occurred and no crystals were formed. When the gas−liquid flow ratio was 8:1, the end point pH_R was 11.86, and almost no solids were produced immediately after the reaction. However, bayerite crystals formed after standing at room temperature for 0.5 h. As the gas−liquid flow ratio further increased, the carbonation reaction rate accelerated. At a gas−liquid flow ratio of 12:1, the end point pH_R of the carbonation reaction was 10.87, resulting in the formation of amorphous aluminum hydroxide, which transformed into bayerite crystals after standing at room temperature for 0.5 h. It was worth noting that the molar ratio of carbon dioxide to sodium aluminate in experiment 22 was equal to that in experiment 11, yet the end point pH_R of the carbonation reaction in experiment 22 was higher than that in experiment 11. This indicated that a larger gas volume in experiment 22 was unfavorable for the carbonation reaction and decreased the utilization efficiency of carbon dioxide. The results demonstrated that increasing the gas−liquid flow ratio could enhance the carbonation reaction rate, promote the decomposition of aluminate ions, and form amorphous aluminum hydroxide nuclei. By adjusting the gas−liquid flow ratio, the nucleation of aluminum hydroxide generated in the carbonation reaction in the high gravity reactor could be controlled.

3.1.4. Influence of the Number of Reactions on Reaction End Point pH and Crystal Phase. Using 40% carbon dioxide gas, a single-stage high gravity reactor could not achieve the appropriate carbonation reaction end point necessary for the growth of pseudoboehmite. Consequently, it was impossible to continuously produce pseudoboehmite from a 0.1 mol/L sodium aluminate solution. Even higher concentrations of sodium aluminate solution failed to achieve continuous production of pseudoboehmite with a single-stage high gravity reactor. This limitation was due to the kinetics of the carbonation reaction and the decomposition reaction of sodium aluminate. The reaction time in the high gravity reactor was extremely short, approximately on the order of seconds.[55] Therefore, a multistage high gravity reactor in series was proposed to intensify the carbonation reaction, enabling the continuous production of pseudoboehmite using flue gas.

The study examined the necessary number of reactions and gas−liquid flow ratios for the continuous production of pseudoboehmite from sodium aluminate solutions of various concentrations. The experimental conditions and results for the number of reactions are shown in Table 4. The effect of the number of reactions on the end point pH_R of the carbonation reaction is illustrated in Figure 10, while the XRD and FTIR characterization results of the crystal phase are presented in Figure 11. A 0.1 mol/L sodium aluminate solution reached an end point pH of 10.3 after two passes through the high gravity

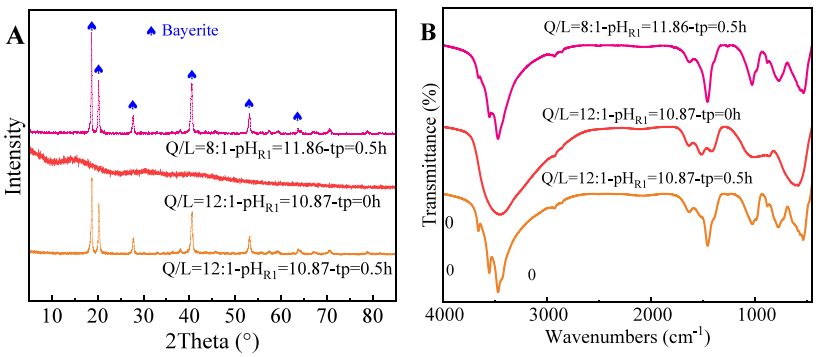

Figure 9. XRD pattern and FTIR spectra of precipitation generated by carbonation reaction (gas−liquid flow ratio). (A) XRD pattern. (B) FTIR spectra.

https://doi.org/10.1021/acsomega.4c05591
ACS Omega 2024, 9, 43570−43582

Table 4. Experimental Result Table of the Effect of the Gas−Liquid Flow Ratio on Carbonation Reaction End Point pH_R and Crystals[a]

numbers	c_{NaAlO_2}/(mol/L)	pH_0	β	ϕ_{CO_2}/%	Q/L	L/(mL/min)	pH_{R1}	pH_{R2}	pH_{R3}	t_p/h	crystalline phase
29	0.1	12.93	80	40	12:1	500	10.87 ± 0.02	10.30 ± 0.03	\	0.5	AA
30	0.1	12.93	80	40	12:1	500	10.87 ± 0.02	10.30 ± 0.03	9.89 ± 0.01	0.5	AA
31	0.2	13.21	80	40	15:1	500	12.16 ± 0.02	11.05 ± 0.03	10.52 ± 0.02	0.5	AA
32	0.3	13.35	80	40	20:1	500	12.48 ± 0.01	11.26 ± 0.01	10.70 ± 0.02	0.5	AA
33	0.4	13.56	80	40	30:1	500	12.94 ± 0.02	11.52 ± 0.02	11.03 ± 0.01	0.5	AA
34	0.5	13.65	80	40	40:1	500	13.12 ± 0.02	11.97 ± 0.02	11.42 ± 0.02	0.5	B

[a]pH_{R2}: reaction end point of the second reactor; pH_{R3}: reaction end point of the third reactor.

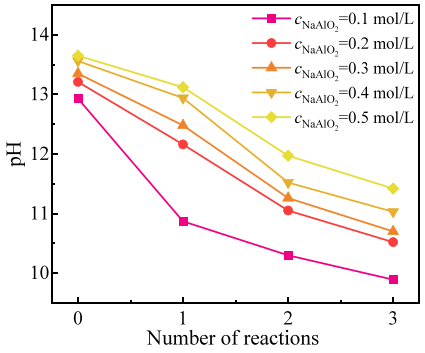

Figure 10. Effect of the number of reactions on carbonation reaction end point pH_R.

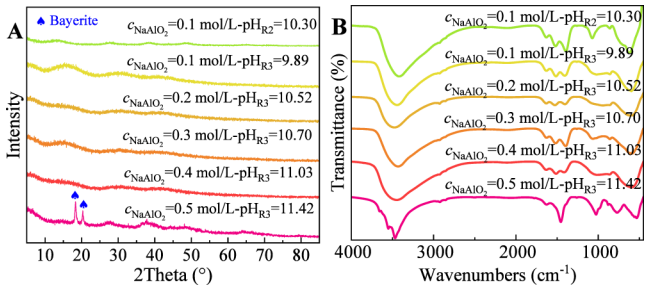

Figure 11. XRD pattern and FTIR spectra of precipitation generated by carbonation reaction (number of reactions). (A) XRD pattern. (B) FTIR spectra.

reactor. At a gas−liquid flow ratio of 15:1, a 0.2 mol/L sodium aluminate solution reached an end point pH of 10.52 after three passes. Similarly, with a gas−liquid flow ratio of 20:1, a 0.3 mol/L sodium aluminate solution achieved an end point pH of 10.70 after three passes. When the gas−liquid flow ratio was 30:1, a 0.4 mol/L sodium aluminate solution reached an end point pH of 11.03 after three passes. Finally, with a gas−liquid flow ratio of 40:1, a 0.5 mol/L sodium aluminate solution reached an end point pH of 11.42 after three passes. The results indicated that sodium aluminate solutions with concentrations below 0.5 mol/L produced amorphous aluminum hydroxide after three passes through the high gravity reactor. However, a 0.5 mol/L sodium aluminate solution produced bayerite crystals after three passes, making it impossible to produce pseudoboehmite with high peptization performance.

3.2. High Gravity-Enhanced Steam Heat Transfer for Continuous Aging to Synthesize Pseudoboehmite Crystals. Amorphous aluminum hydroxide nuclei produced by the high gravity carbonation reaction underwent aging treatment. For the first time, a high gravity steam heating device was introduced, enabling simultaneous heat and mass transfer between the feed liquid and steam. The feed liquid was instantaneously heated to the aging temperature within seconds. Following heating, the feed liquid was maintained at the aging temperature and allowed to flow through the aging pipeline for a specified duration. The crystal phases formed under different carbonation reaction end points, aging temperatures, and aging times were examined. The synthesis conditions and results are listed in Table 5. The XRD and FTIR spectra are shown in Figures 12 and 13, respectively.

Table 5. Experimental Results of the Effect of Heating Rate and Carbon Fraction Reaction End Point on Precipitation[a]

number	c_{NaAlO_2}/(mol/L)	pH_R	t_p/h	T_A/°C	t_A/h	crystal phase
8-90-3	0.1	10.13	0	90	3	PB
29-90-3	0.1	10.30	0	90	3	PB
18-90-3	0.1	10.50	0	90	3	PB + B
25-90-3	0.1	10.87	0	90	3	PB + B
4-90-3	0.1	11.28	0	90	3	PB + B + G
16-90-3	0.1	11.67	0	90	3	B + G
22-90-3	0.1	11.87	0	90	3	B + G
31-90-3	0.2	10.52	0	90	3	PB
32-90-3	0.3	10.70	0	90	3	PB
34-90-3	0.5	11.42	0	90	3	PB + B
33-30-3	0.4	11.03	0	30	3	LC-PB
33-50-3	0.4	11.03	0	50	3	LC-PB
33-70-3	0.4	11.03	0	70	3	PB
33-90-0.5	0.4	11.03	0	90	0.5	PB
33-90-1	0.4	11.03	0	90	1	PB
33-90-2	0.4	11.03	0	90	2	PB
33-90-3	0.4	11.03	0	90	3	PB

[a]Number *X-Y-Z*: *X* is the reaction number in Section 3.1, *Y* is the aging temperature, and *Z* is the aging time; T_A: aging temperature (°C); t_H: aging time (h); PB: pseudoboehmite; G: gibbsite; LC: low crystallinity.

After aging, amorphous aluminum hydroxide formed at lower carbonation reaction end points transformed into pseudoboehmite, as shown in experiments 8-90-3 and 29-90-3 in Table 4. This indicates that amorphous aluminum hydroxide serves as the precursor to pseudoboehmite. At higher carbonation reaction end points, amorphous aluminum hydroxide rapidly grew into pseudoboehmite, with bayerite also appearing swiftly, as demonstrated in experiments 18-90-3, 25-90-3, and 4-90-3 in Table 4. Zhang et al.[26] reported that pseudoboehmite grew into bayerite. This suggests that rapidly increasing the temperature not only accelerates the transformation of amorphous aluminum hydroxide into pseudoboehmite but also promotes the nucleation and growth of

https://doi.org/10.1021/acsomega.4c05591
ACS Omega 2024, 9, 43570−43582

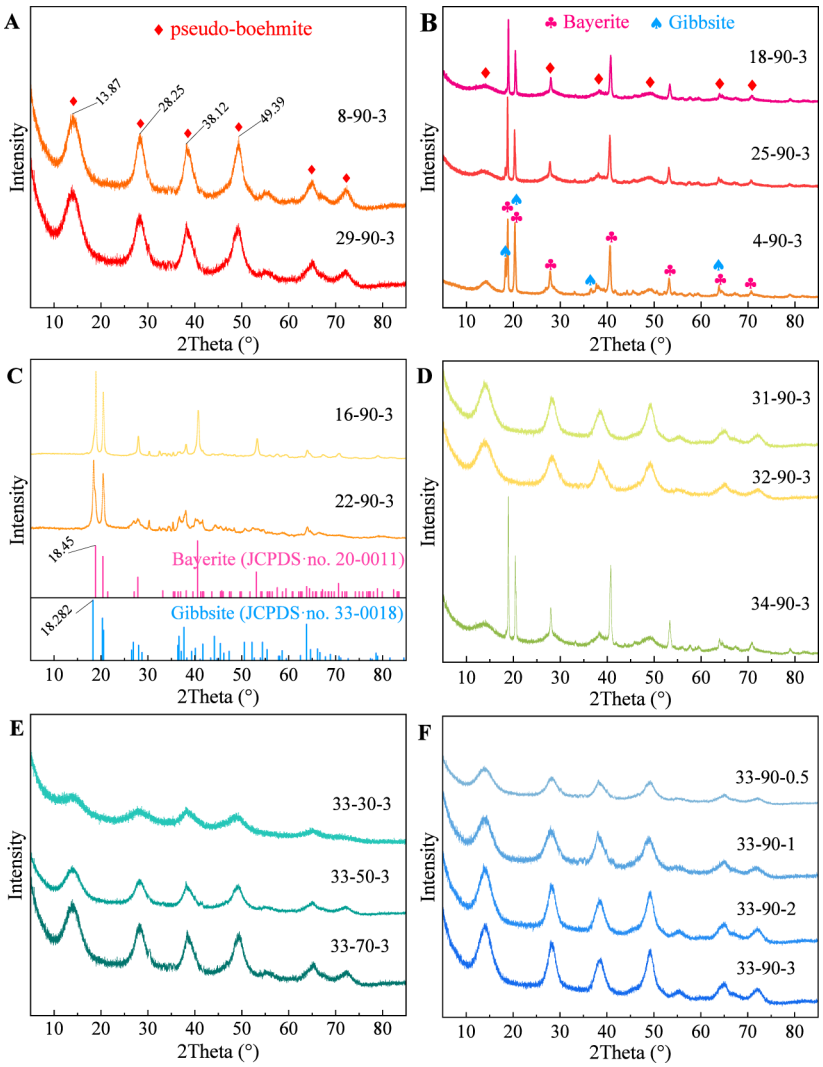

Figure 12. XRD pattern of precipitation generated by aging. (A) The experiments were 8-90-3 and 29-90-3. (B) The experiments were 18-90-3, 25-90-3, and 4-90-3. (C) The experiments were 16-90-3 and 22-90-3. (D) The experiments were 31-90-3, 32-90-3, and 34-90-3. (E) The experiments 33-30-3, 33-50-3, and 33-70-3. (F) The experiments were 33-90-0.5, 33-90-1, 33-90-2, and 33-90-3.

bayerite. When the carbonation reaction end point was very high, no amorphous aluminum hydroxide was formed, and the growth of bayerite into gibbsite was expedited, as observed in experiments 16-90-3 and 22-90-3 in Table 4. Both XRD and FTIR spectra exhibited consistent results. Zolfaghari et al.[56] reported that bayerite grew as gibbsite and its XRD and FTIR spectra.

Using three high gravity reactors, continuous production of pseudoboehmite was achieved from 0.2, 0.3, and 0.4 mol/L sodium aluminate solutions with 40% carbon dioxide gas, as shown in experiments 31-90-3, 32-90-3, and 33-90-3 in Table 4, respectively. However, under the same experimental conditions, continuous production of pseudoboehmite from a 0.5 mol/L sodium aluminate solution was not successful, as indicated by experiment 34-90-3.

The effects of different aging temperatures and durations on the pseudoboehmite crystals formed from a 0.4 mol/L sodium aluminate solution were investigated. The experimental conditions and results are detailed in Table 4, covering experiments 33-30-3, 33-50-3, 33-70-3, 33-90-0.5, 33-90-1, 33-90-2, and 33-90-3. Increasing the aging temperature and duration gradually enhanced the crystallinity of the pseudoboehmite, as shown in Figure 11E,F. The thermal analysis curves of pseudoboehmite (33-90-3) and bayerite (18-90-3) are shown in Figure 14. The thermal analysis curves of the two are completely different. The heat loss of pseudoboehmite can be divided into three stages, that is, three different crystal structures appear. The heat loss of bayerite is divided into two stages, that is, two different crystal structures appear.

The research results indicated that the rapid heating and aging process in a high gravity environment accelerated the crystal growth rate of pseudoboehmite, reducing the heating time from 0.5 h to a few seconds. Furthermore, the experiments demonstrated that integrating three high gravity reactors with one high gravity aging unit enabled the continuous production of pseudoboehmite.

3.3. Influence of Synthesis Conditions on the Peptizing Ability of Pseudoboehmite. The influence of different synthesis conditions on the peptizing ability of pseudoboehmite is shown in Figure 15. The peptization index of pseudoboehmite increased with increasing aging temperature and time. The carbonation reaction end point pH that pseudoboehmite only was generated had no effect on the peptization index, as shown in Figure 15C. When the end point

https://doi.org/10.1021/acsomega.4c05591
ACS Omega 2024, 9, 43570−43582

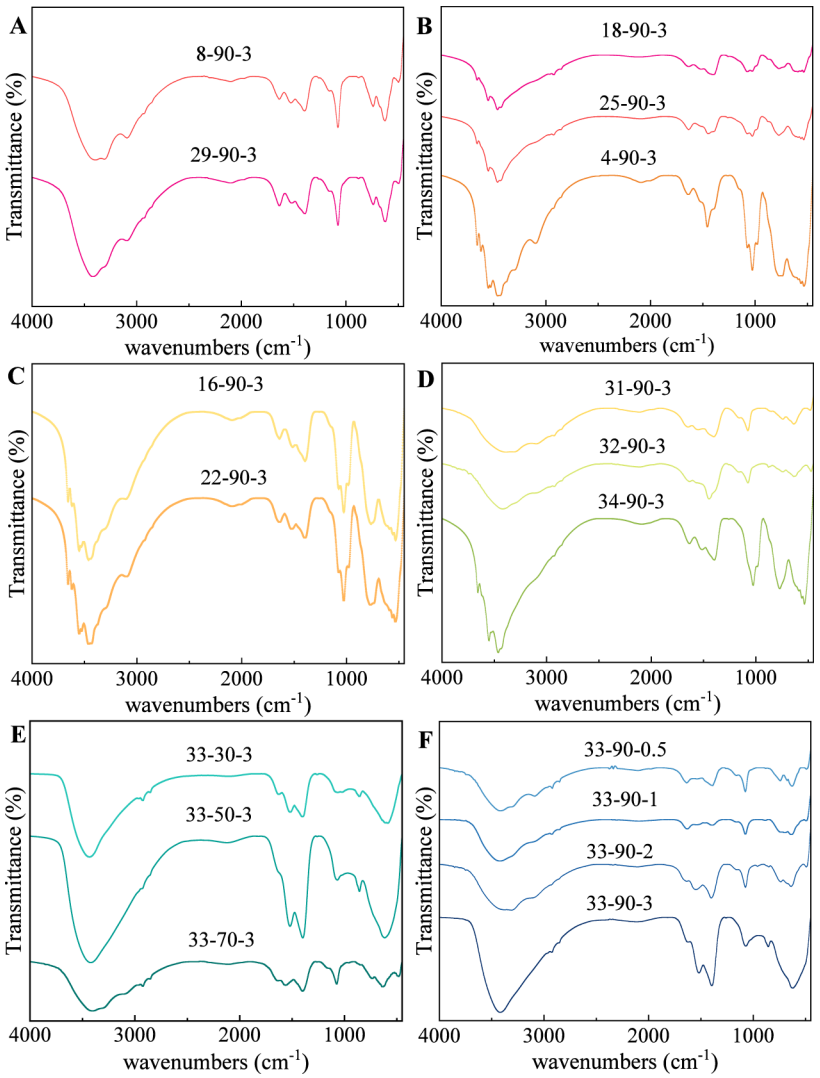

Figure 13. FTIR spectra of precipitate generated by aging. (A) The experiments were 8-90-3 and 29-90-3. (B) The experiments were 18-90-3, 25-90-3, and 4-90-3. (C) The experiments were 16-90-3 and 22-90-3. (D) The experiments were 31-90-3, 32-90-3, and 34-90-3. (E) The experiments were 33-30-3, 33-50-3, and 33-70-3. (F) The experiments were 33-90-0.5, 33-90-1, 33-90-2, and 33-90-3.

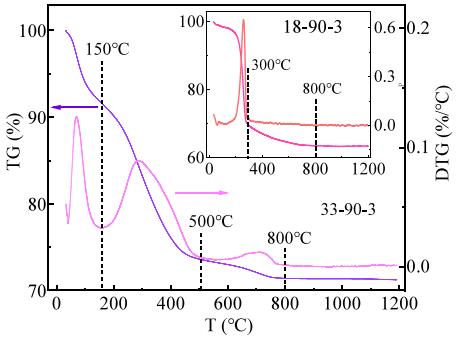

Figure 14. TG curves of pseudoboehmite and bayerite.

pH of carbonation reaction was high, the formation of bayerite seriously affected the peptization index. The concentration of sodium aluminate solution had no effect on the peptization index of pseudoboehmite. Under the conditions of rapid carbonation at 25 °C, rapid heating to 90 °C, and aging for 3 h, pseudoboehmite with a peptization index of 100% was prepared by the high gravity method.

3.4. Mechanism of Nucleation and Growth of Pseudoboehmite Crystals Enhanced by High Gravity.

The growth of amorphous aluminum hydroxide and bayerite crystals produced in experiments 6 and 7 was investigated. The morphology of amorphous aluminum hydroxide appeared as spheroidal aggregates (Figure 16), while the morphology of bayerite was conical[29] (Figure 17). In Figure 17A, conical bayerite crystals of varying sizes can be observed, with smaller conical bayerite crystals being the same size as the spheroidal amorphous aluminum hydroxide. Additionally, amorphous aluminum hydroxide and small conical bayerite crystals adhered to the surface of the larger conical bayerite crystals. This indicates that both amorphous aluminum hydroxide and bayerite nuclei nucleate independently, consistent with the secondary decomposition reaction of sodium aluminate reported in ref 41. The small conical bayerite nuclei continuously fused and grew into larger conical structures, a process that aligns with the Ostwald Ripening theory. Influenced by environmental factors and crystal interface stability, amorphous aluminum hydroxide underwent secondary growth into bayerite on the surface of the existing bayerite crystals. After 0.5 h, the size of bayerite increased and the

https://doi.org/10.1021/acsomega.4c05591
ACS Omega 2024, 9, 43570−43582

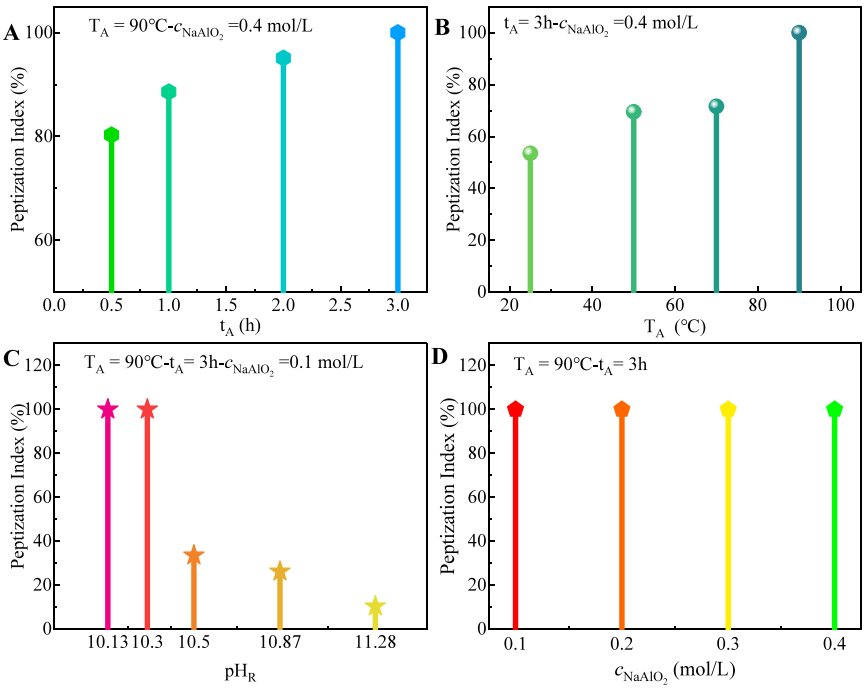

Figure 15. Effect of preparation conditions on the peptizing index of pseudoboehmite. (A) Aging time. (B) Aging temperature. (C) Carbonation reaction end point pH. (D) Concentration of sodium aluminate solution.

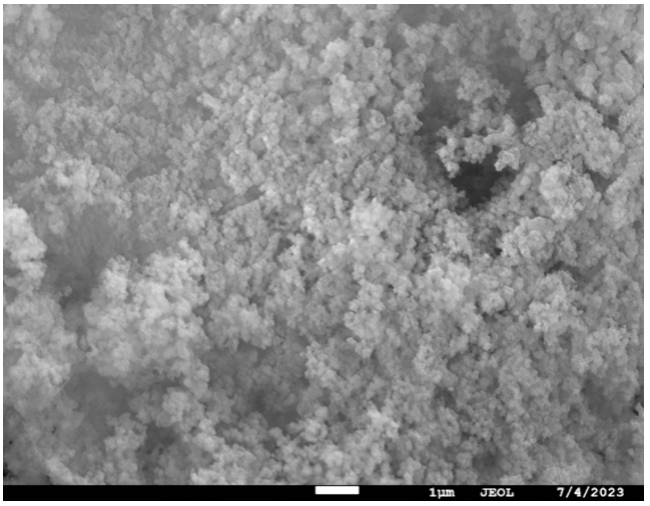

Figure 16. SEM morphology of amorphous aluminum hydroxide.

amount of amorphous aluminum hydroxide decreased (Figure 17). At 90 °C, the conical bayerite dissolved, and in situ growth of various-sized plate-like gibbsite occurred (Figure 18). At higher temperatures, the 100 nm spheroidal amorphous aluminum hydroxide crystals gradually fused and grew into blocky pseudoboehmite crystals larger than 1 μm (Figure 19). With increasing temperature and time, the surface of the pseudoboehmite crystals became progressively smoother and the degree of crystallinity increased. Figure 20 shows the EDS diagram of pseudoboehmite prepared by aging at 90 °C for 1 h, which showed the distribution and relative contents of Al, O, C, and Na elements. The Na element was present because sodium ions in the aqueous solution adhered to the surface of the material. The C element was because the fixed material used is carbon cloth. The distribution of oxygen and aluminum elements was very uniform, and the relative ratio of the amount of matter was 3.68:1. The relative proportion was greater than the elemental proportion (3) of aluminum hydroxide compounds because the material contained a large amount of adsorbed water and crystal water. This also proves

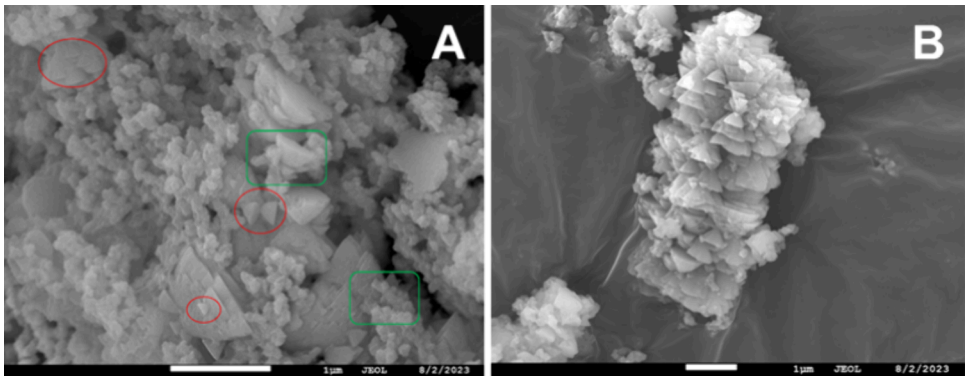

Figure 17. SEM morphology of bayerite generated by pH_{R1} = 11.28 (A: t_p = 0.1 h; B: t_p = 0.5 h).

https://doi.org/10.1021/acsomega.4c05591
ACS Omega 2024, 9, 43570−43582

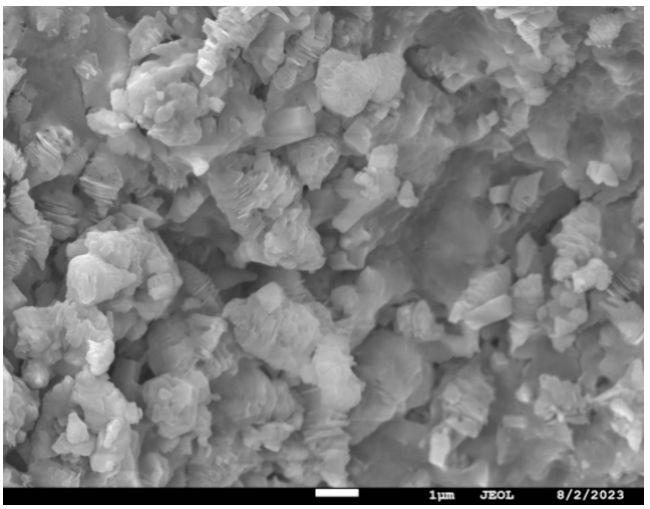

Figure 18. SEM morphology of gibbsite generated by aging at 90 °C for 3 h.

that pseudoboehmite contains more water than aluminum hydroxide.

In the high gravity reactor, the liquid phase is dispersed into small droplets, creating a dispersed phase, while the gas phase serves as the continuous phase. This configuration ensures rapid and uniform attainment of the reaction end point within seconds, promoting the nucleation of pseudoboehmite crystals and preventing the nucleation of bayerite. This is essential for achieving pseudoboehmite with 100% peptization performance. The high gravity steam heating device ensures uniform mixing of steam and feed liquid, enhancing heat and mass transfer. It fully utilizes both the sensible and latent heat of the steam, significantly reducing the heating time of the feed liquid and enabling amorphous aluminum hydroxide to quickly grow into pseudoboehmite. In the aging pipeline, the feed liquid flows continuously, maintaining a more stable temperature, thereby addressing the issues of poor temperature and time uniformity in batch aging devices. This uniform growth of pseudoboehmite crystals eliminates dead zones in crystal growth, significantly improving the peptization performance of pseudoboehmite.

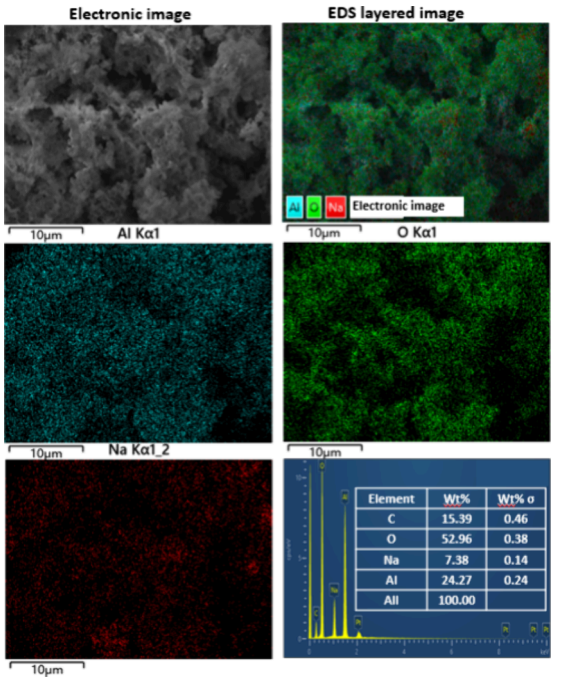

Figure 20. SEM-EDS morphology of pseudoboehmite (Figure 19A).

4. CONCLUSIONS

Increasing the high gravity factor, gas−liquid ratio, and carbon dioxide content accelerates the carbonation reaction rate and enhances the nucleation rate of pseudoboehmite. Connecting multiple high gravity reactors in series extends the reaction time, allowing high-concentration sodium aluminate to quickly reach the carbonation reaction end point and achieve precise control of pseudoboehmite nucleation. This approach addresses the issue of slow carbonation reaction rates that hinder controlled nucleation of pseudoboehmite. The high gravity reactor accelerates the carbonation reaction and precisely controls the reaction end point, reducing the reaction time from minutes to seconds, thereby enhancing pseudoboehmite crystal nucleation and enabling a continuous carbonation reaction process. The high gravity-enhanced

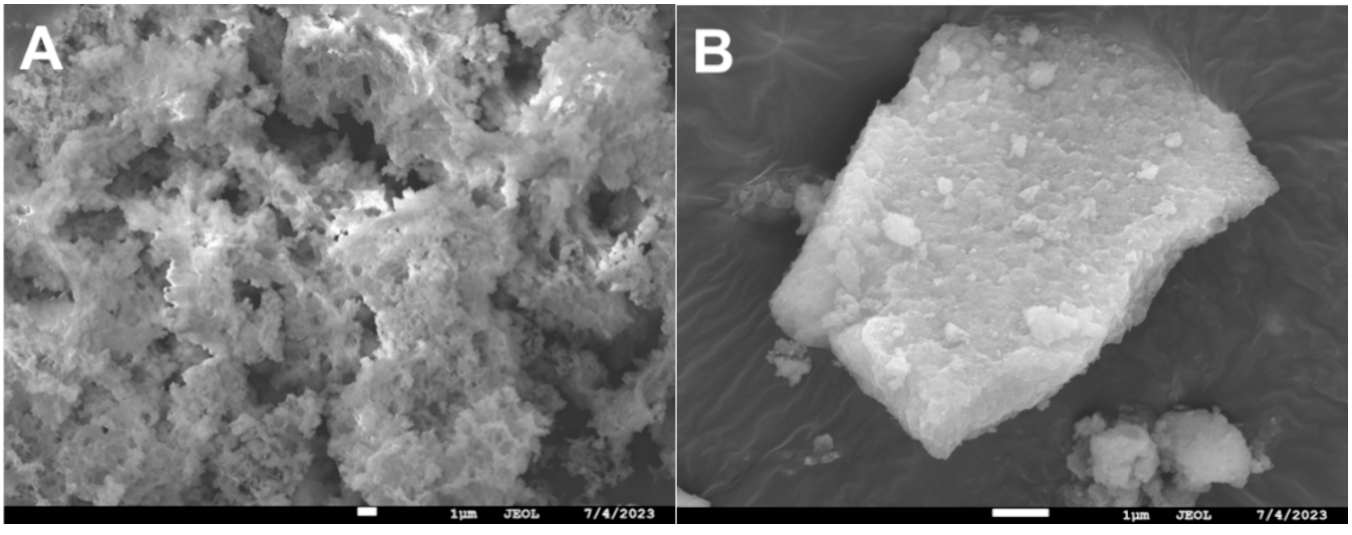

Figure 19. SEM morphology of pseudoboehmite generated by aging at 90 °C (A: 1 h; B: 3 h).

https://doi.org/10.1021/acsomega.4c05591
ACS Omega 2024, 9, 43570−43582

steam heating process rapidly heats the pseudoboehmite feed liquid to the aging temperature, completing the continuous aging process in the aging pipeline. This study achieved continuous production of pseudoboehmite with a peptization index of 100% from a 0.4 mol/L sodium aluminate solution, providing a novel preparation process for aluminum hydroxide and significantly improving production efficiency. The proposed whole process continuous preparation method can be extended to the research and production of other powders.

■ ASSOCIATED CONTENT

Data Availability Statement

All data could be found in the experimental part.

■ AUTHOR INFORMATION

Corresponding Author

Youzhi Liu − *School of Chemistry and Chemical Engineer, North University of China, Taiyuan 030051, China; Shanxi Province Key Laboratory of Chemical Process Intensification, Taiyuan 030051, China*; Email: liuyz@nuc.edu.cn

Authors

Chengqian Zhang − *School of Chemistry and Chemical Engineer, North University of China, Taiyuan 030051, China; Shanxi Province Key Laboratory of Chemical Process Intensification, Taiyuan 030051, China*; orcid.org/0009-0005-1103-6409

Yuliang Li − *School of Chemistry and Chemical Engineer, North University of China, Taiyuan 030051, China; Shanxi Province Key Laboratory of Chemical Process Intensification, Taiyuan 030051, China*

Shuwei Guo − *School of Chemistry and Chemical Engineer, North University of China, Taiyuan 030051, China; Shanxi Province Key Laboratory of Chemical Process Intensification, Taiyuan 030051, China*

Shufei Wang − *School of Chemistry and Chemical Engineer, North University of China, Taiyuan 030051, China; Shanxi Province Key Laboratory of Chemical Process Intensification, Taiyuan 030051, China*

Shangyuan Cheng − *School of Chemistry and Chemical Engineer, North University of China, Taiyuan 030051, China; Shanxi Province Key Laboratory of Chemical Process Intensification, Taiyuan 030051, China*

Complete contact information is available at: https://pubs.acs.org/10.1021/acsomega.4c05591

Notes

The authors declare no competing financial interest.

■ ACKNOWLEDGMENTS

We thank the National Natural Science Foundation of China (General Program, 22378370 and 22108263) and the Natural Science Foundation of Shanxi Province (20210302124060) for the funding support of this research.

■ REFERENCES

(1) Tian, K.; Li, Q.; Jiang, W.; Wang, X.; Liu, S.; Zhao, Y.; Zhou, G. Effect of the pore structure of an active alumina catalyst on isobutene production by dehydration of isobutanol. *RSC Adv.* **2021**, *11* (20), 11952−11958.

(2) Liu, Y.; Qing, S.; Hou, X.; Qin, F.; Wang, X.; Gao, Z.; Xiang, H. Temperature dependence of Cu−Al spinel formation and its catalytic performance in methanol steam reforming. *Catalysis Science & Technology* **2017**, *7* (21), 5069−5078.

(3) Schacht, P.; Ramírez, S.; Ancheyta, J. CoMo/Ti-MCM-41/Alumina Catalysts: Properties and Activity in the Hydrodesulfurization (HDS) of Dibenzothiophene (DBT). *Energy Fuels* **2009**, *23* (10), 4860−4865.

(4) Kong, D.; Liu, Y.; Zhang, J.; Li, H.; Wang, X.; Liu, G.; Li, B.; Xu, Z. Hierarchically porous AlPO-5-based microspheres as heterogeneous catalysts for the synthesis of 5-substituted 1H-tetrazoles via [3 + 2] cycloaddition. *New J. Chem.* **2014**, *38* (7), 3078−3083.

(5) Liu, Y.; Lyu, Y.; Zhao, X.; Xu, L.; Mintova, S.; Yan, Z.; Liu, X. Silicoaluminophosphate-11 (SAPO-11) molecular sieves synthesized via a grinding synthesis method. *Chem. Commun.* **2018**, *54* (78), 10950−10953.

(6) Yao, J.; Rong, Y.; Gao, Z.; Tang, X.; Zha, F.; Tian, H.; Chang, Y.; Guo, X. Metal−organic framework-assisted synthesis of Zr-modified SAPO-34 zeolites with hierarchical porous structure for the catalytic transformation of methanol to olefins. *Catalysis Science & Technology* **2022**, *12* (3), 894−905.

(7) Auxilio, A. R.; Andrews, P. C.; Junk, P. C.; Spiccia, L.; Neumann, D.; Raverty, W.; Vanderhoek, N.; Pringle, J. M. Functionalised pseudo-boehmite nanoparticles as an excellent adsorbent material for anionic dyes. *J. Mater. Chem.* **2008**, *18* (21), 2466−2474.

(8) Liang, L.; Mi, J.; Li, L.; He, X.; Guo, W. Mesoporous adsorbent for competitive adsorption of fluoride ions in zinc sulfate solution. *RSC Adv.* **2021**, *11* (22), 13521−13529.

(9) Li, S.; Shi, Y.; Cai, N. Potassium-Promoted γ-Alumina Adsorbent from K2CO3 Coagulated Alumina Sol for Warm Gas Carbon Dioxide Separation. *ACS Sustainable Chem. Eng.* **2015**, *3* (1), 111−116.

(10) Zhang, H.; Li, P.; Wang, Z.; Zhang, X.; Zheng, S.; Zhang, Y. In Situ Synthesis of γ-AlOOH and Synchronous Adsorption Separation of V(V) from Highly Concentrated Cr(VI) Multiplex Complex solutions. *ACS Sustainable Chem. Eng.* **2017**, *5* (8), 6674−6681.

(11) Kharabe, G. P.; Manna, N.; Nadeema, A.; Singh, S. K.; Mehta, S.; Nair, A.; Joshi, K.; Kurungot, S. A pseudo-boehmite AlOOH supported NGr composite-based air electrode for mechanically rechargeable Zn-air battery applications. *Journal of Materials Chemistry A* **2022**, *10* (18), 10014−10025.

(12) Ma, H.; Yu, Z.; Chen, J.; Wang, D.; Dong, C.; Mao, Z. Incorporating α-Al2O3 Nanodots into Expanded Graphite Anodes toward Stable Fast Charging for Lithium-Ion Batteries. *ACS Applied Energy Materials* **2023**, *6* (3), 1389−1395.

(13) Colaprico, A.; Senesi, S.; Ferlicca, F.; Brunelli, B.; Ugozzoli, M.; Pallaoro, M.; O'Hagan, D. T. Adsorption onto aluminum hydroxide adjuvant protects antigens from degradation. *Vaccine* **2020**, *38* (19), 3600−3609.

(14) Glenny, A. T.; Pope, C. G.; Waddington, H.; Wallace, U. Immunological notes. XXIII. The antigenic value of toxoid precipitated by potassium alum. *Journal of Pathology and Bacteriology* **1926**, *29* (1), 31−40.

(15) Li, H.; Nookala, S.; Re, F. Aluminum Hydroxide Adjuvants Activate Caspase-1 and Induce IL-1β and IL-18 Release. *J. Immunol.* **2007**, *178* (8), 5271−5276.

(16) Marrack, P.; McKee, A. S.; Munks, M. W. Towards an understanding of the adjuvant action of aluminium. *Nature Reviews Immunology* **2009**, *9* (4), 287−293.

(17) Zhao, Y.; Xi, C.; Gao, S.; Wang, Y.; Wang, H.; Sun, P.; Wu, Z. Ru-based monolithic catalysts for the catalytic oxidation of chlorinated volatile organic compounds. *RSC Adv.* **2023**, *13* (10), 7037−7044.

(18) Sinha Majumdar, S.; Celik, G.; Ozkan, U. S. Investigation of the Effect of Alumina Binder Addition to Pd/SO42−−ZrO2 Catalysts during Sol−Gel Synthesis. *Ind. Eng. Chem. Res.* **2016**, *55* (44), 11445−11457.

(19) Azadi, P.; Afif, E.; Azadi, F.; Farnood, R. Screening of nickel catalysts for selective hydrogen production using supercritical water gasification of glucose. *Green Chem.* **2012**, *14* (6), 1766−1777.

(20) Handjani, S.; Blanchard, J.; Marceau, E.; Beaunier, P.; Che, M. From mesoporous alumina to Pt/Al2O3 catalyst: A comparative study

https://doi.org/10.1021/acsomega.4c05591
ACS Omega 2024, 9, 43570−43582

of the aluminas synthesis in aqueous medium, physicochemical properties and stability. *Microporous Mesoporous Mater.* **2008**, *116* (1−3), 14−21.
(21) Lu, G.; Zhang, T.; Feng, W.; Zhang, W.; Wang, Y.; Zhang, Z.; Wang, L.; Liu, Y.; Dou, Z. Preparation and Properties of Pseudo-boehmite Obtained from High-Alumina Fly Ash by a Sintering−CO2 Decomposition Process. *Jom* **2019**, *71* (2), 499−507.
(22) Ren, X.; Liu, Y.; Miao, L. Continuous Carbonation for Synthesis of Pseudo-Boehmite by using Cross-Flow Rotating Packed Bed through the Reaction of NaAlO2 Solution with CO2 Gas. *Nanomaterials (Basel)* **2020**, *10* (2), 263.
(23) Wang, Y.; Xu, D.; Sun, H.; Luo, G. Preparation of Pseudoboehmite with a Large Pore Volume and a Large Pore Size by Using a Membrane-Dispersion Microstructured Reactor through the Reaction of CO2 and a NaAlO2 Solution. *Ind. Eng. Chem. Res.* **2011**, *50* (7), 3889−3894.
(24) Liu, C.; Li, J.; Liew, K.; Zhu, J.; Nordin, M. R. b. An environmentally friendly method for the synthesis of nano-alumina with controllable morphologies. *RSC Adv.* **2012**, *2* (22), 8352−8358.
(25) Yang, F.; Wang, Q.; Yan, J.; Fang, J.; Zhao, J.; Shen, W. Preparation of High Pore Volume Pseudoboehmite Doped with Transition Metal Ions through Direct Precipitation Method. *Ind. Eng. Chem. Res.* **2012**, *51* (47), 15386−15392.
(26) Zhang, H.; Zhang, X.; Graham, T. R.; Pearce, C. I.; Hlushko, H.; LaVerne, J. A.; Liu, L.; Wang, S.; Zheng, S.; Zhang, Y.; Clark, S. B.; Li, P.; Wang, Z.; Rosso, K. M. Crystallization and Phase Transformations of Aluminum (Oxy)hydroxide Polymorphs in Caustic Aqueous Solution. *Inorg. Chem.* **2021**, *60* (13), 9820−9832.
(27) Majhi, A.; Pugazhenthi, G.; Shukla, A. Comparative study of ultrasound stimulation and conventional heating methods on the preparation of nanosized γ-Al2O3. *Ind. Eng. Chem. Res.* **2010**, *49*, 4710−4719.
(28) Du, X.; Wang, Y.; Su, X.; Li, J. Influences of pH value on the microstructure and phase transformation of aluminum hydroxide. *Powder Technol.* **2009**, *192* (1), 40−46.
(29) Jiang, Y.-F.; Liu, C.-L.; Xue, J.; Li, P.; Yu, J.-G. Insights into the polymorphic transformation mechanism of aluminum hydroxide during carbonation of potassium aluminate solution. *CrystEngComm* **2018**, *20* (10), 1431−1442.
(30) Cai, W.; Li, H.; Zhang, G. Enhancement on Synthesis of Boehmite Through a Precarbonization-assisted Hydrogen Peroxide Route in Highly Alkaline Sodium Aluminate Solutions. *Chinese Journal of Chemical Engineering* **2010**, *18* (3), 500−505.
(31) Wang, Z.; Du, H.; Gong, J.; Yang, S.; Ma, J.; Xu, J. Facile synthesis of hierarchical flower-like γ-AlOOH films via hydrothermal route on quartz surface. *Colloids Surf., A* **2014**, *450*, 76−82.
(32) Asadi, A. A.; Alavi, S. M.; Royaee, S. J.; Bazmi, M. Ultra-deep Hydrodesulfurization of Feedstock Containing Cracked Gasoil through NiMo/γ-Al2O3 Catalyst Pore Size Optimization. *Energy Fuels* **2018**, *32* (2), 2203−2212.
(33) Asadi, A. A.; Bazmi, M.; Alavi, S. M.; Royaee, S. J. Neutralization of NaAlO2 solution with CO2 for synthesis of γ-Al2O3 nanoparticles, part 1: effects of synthesis parameters in semi-batch membrane dispersion microstructured reactor. *RSC Adv.* **2016**, *6* (111), 109681−109691.
(34) Wan, Y.; Liu, Y.; Wang, Y.; Luo, G. Preparation of Large-Pore-Volume γ-Alumina Nanofibers with a Narrow Pore Size Distribution in a Membrane Dispersion Microreactor. *Ind. Eng. Chem. Res.* **2017**, *56* (31), 8888−8894.
(35) Yang, Y.; Xu, Y.; Han, B.; Xu, B.; Liu, X.; Yan, Z. Effects of synthetic conditions on the textural structure of pseudo-boehmite. *J. Colloid Interface Sci.* **2016**, *469*, 1−7.
(36) Balakrishnan, K.; Gonzalez, R. D. Preparation of Bimetallic Pt-Sn/Alumina Catalysts by the Sol-Gel Method. *Langmuir* **1994**, *10* (7), 2487−2490.
(37) Fulvio, P. F.; Brosey, R. I.; Jaroniec, M. Synthesis of Mesoporous Alumina from Boehmite in the Presence of Triblock Copolymer. *ACS Appl. Mater. Interfaces* **2010**, *2* (2), 588−593.
(38) Wang, Z.-M.; Lin, Y. S. Sol−Gel-Derived Alumina-Supported Copper Oxide Sorbent for Flue Gas Desulfurization. *Ind. Eng. Chem. Res.* **1998**, *37* (12), 4675−4681.
(39) Mukhamed'yarova, A. N.; Egorova, S. R.; Nosova, O. V.; Lamberov, A. A. Influence of hydrothermal conditions on the phase transformations of amorphous alumina. *Mendeleev Commun.* **2021**, *31* (3), 385−387.
(40) Czajkowski, A.; Noworyta, A.; Krótki, M. Studies and modelling of the process of decomposition of aluminate solutions by carbonation. *Hydrometallurgy* **1981**, *7* (3), 253−261.
(41) Zhang, C.; Liu, Y.; Li, Y.; Guo, S.; Wang, S.; Cheng, S.; Shen, H. Study on Controlled Synthesis of Mesoporous Pseudoboehmite via Carbonation Reaction. *Ind. Eng. Chem. Res.* **2024**, *63* (13), 5655−5665.
(42) Ren, X.; Liu, Y.; Miao, L. Continuous Carbonation for Synthesis of Pseudo-Boehmite by using Cross-Flow Rotating Packed Bed through the Reaction of NaAlO(2) Solution with CO(2) Gas. *Nanomaterials (Basel)* **2020**, *10* (2), 263.
(43) Chen, J.-F.; Shao, L.; Guo, F.; Wang, X.-M. Synthesis of nano-fibers of aluminum hydroxide in novel rotating packed bed reactor. *Chem. Eng. Sci.* **2003**, *58* (3−6), 569−575.
(44) Shayanfar, S.; Aghazadeh, V.; Saravari, A.; Hasanpour, P. Aluminum hydroxide crystallization from aluminate solution using carbon dioxide gas: Effect of temperature and time. *J. Cryst. Growth* **2018**, *496−497*, 1−9.
(45) Shayanfar, S.; Aghazadeh, V.; Samiee Beyragh, A. Thermodynamic Modeling and Experimental Studies of Bayerite Precipitation from Aluminate Solution Temperature and pH Effect. *Iran. J. Chem. Chem. Eng.* **2019**, *38* (2), 229.
(46) Liu, C.-L.; Jiang, Y.-F.; Wang, D.; Song, X.-F.; Yu, J.-G. Utilization of CO2 as carbon source for preparation of sandy Al(OH)(3) in concentrated KAl(OH)(4) solutions: a kinetic study. *Energy Sources Part a-Recovery Utilization and Environmental Effects* **2019**, *41* (20), 2507−2518.
(47) Marinos, D.; Kotsanis, D.; Alexandri, A.; Balomenos, E.; Panias, D. Carbonation of Sodium Aluminate/Sodium Carbonate Solutions for Precipitation of Alumina Hydrates-Avoiding Dawsonite Formation. *Crystals* **2021**, *11* (7), 836.
(48) Mwase, J. M.; Vafeias, M.; Marinos, D.; Dimitrios, P.; Safarian, J. Investigating Aluminum Tri-Hydroxide Production from Sodium Aluminate Solutions in the Pedersen Process. *Processes* **2022**, *10* (7), 1370.
(49) Wang, D.; Guo, F.; Chen, J.; Liu, H.; Zhang, Z. Preparation of nano aluminium trihydroxide by high gravity reactive precipitation. *Chemical Engineering Journal* **2006**, *121* (2−3), 109−114.
(50) Wang, D.-G.; Guo, F.; Chen, J.-F.; Shao, L.; Liu, H.; Zhang, Z.-T. A two-step way to synthesize nano inner-modified aluminum trihydroxide. *Colloids and Surfaces a-Physicochemical and Engineering Aspects* **2007**, *293* (1−3), 201−209.
(51) Liu, Y.Chapter 1 - Introduction. In *HiGee Chemical Separation Engineering*; Liu, Y., Ed. Elsevier: 2024, pp 1−22.
(52) Guo, S.; Liu, Y.; Zhang, C.; Zhang, C.; Wang, S.; Li, Y.; Cheng, S. Computational Fluid Dynamics Analysis of Wet Dust Removal in High-Gravity Countercurrent Rotating Packed Bed. *Atmosphere* **2024**, *15* (2), 157.
(53) Lefvre, G.; Ḟdoroff, M. Synthesis of bayerite (β-Al(OH)3) microrods by neutralization of aluminate ions at constant pH. *Mater. Lett.* **2002**, *56*, 978−983.
(54) Jraba, N.; Tounsi, H.; Makhlouf, T. Valorization of Aluminum Chips into γ-Al2O3 and η-Al2O3 with High Surface Areas via the Precipitation Route. *Waste and Biomass Valorization* **2018**, *9* (6), 1003−1014.
(55) Liu, Y.Chapter 2 - Absorption. In *HiGee Chemical Separation Engineering*; Liu, Y., Ed. Elsevier: 2024, pp 23−74.
(56) Zolfaghari, R.; Rezai, B.; Bahri, Z.; Mahmoudian, M. Influences of New Synthesized Active Seeds and Industrial Seed on the Aluminum Hydroxide Precipitation from Sodium Aluminate Solution. *Journal of Sustainable Metallurgy* **2020**, *6* (4), 643−658.

https://doi.org/10.1021/acsomega.4c05591
ACS Omega 2024, 9, 43570−43582